Title

Streptococcus pyogenes M1T1 variants induce an inflammatory phenotype in neutrophils

Authors/Affiliations

Jonathan G. Williams[1,2], Diane Ly[1,2], Nicholas J. Geraghty[1,2], Jason D. McArthur[1,2], Heema K. N. Vyas[1,2], Jody Gorman[1,2], James A. Tsatsaronis[3], Ronald Sluyter[1,2], Martina L. Sanderson-Smith[1,2,4,*]

[1]Illawarra Health and Medical Research Institute, Wollongong, New South Wales, Australia.

[2]Molecular Horizons and School of Chemistry and Molecular Bioscience, University of Wollongong, Wollongong, New South Wales, Australia.

[3]College of Science, Health and Engineering, La Trobe University, Bundoora, Victoria, Australia.

[4]Lead contact

Contact Info

*Correspondence: Illawarra Health and Medical Research Institute (IHMRI), School of Chemistry and Molecular Bioscience, University of Wollongong, Wollongong, NSW, 2522, Australia. E-mail: martina@uow.edu.au

Summary

Invasive infections due to Group A *Streptococcus* (GAS) advance rapidly causing tissue degradation and unregulated inflammation. Neutrophils are the primary immune cells that respond to GAS. M1T1 GAS isolate 5448 and animal passaged variant 5448AP, containing a *covS* mutation, were assessed for their influence on neutrophils. 5448AP proliferated during neutrophil co-incubation and induced lower neutrophil reactive oxygen species production when compared with 5448. Infection with both strains invoked neutrophil death, however apoptosis was reduced in response to 5448AP. Both strains induced neutrophil caspase-1 activation *in vitro*, and elicited IL-1β and TNF-α release from neutrophils. GAS infection altered the cell-surface

expression of CD16 and CD31 on neutrophils. *In vivo* mouse studies confirmed activation of caspase-1 in neutrophils, while 5448AP infection increased circulating IL-1β. GAS infections that promote an inflammatory neutrophil phenotype may contribute to increased inflammation yet ineffective bacterial eradication, contributing to the severity of invasive GAS infections.

Keywords

Polymorphonuclear leukocyte, PMN, apoptosis, pyroptosis, caspase-1, caspase-3, caspase-4, IL-1β, TNF-α, IL-8, IL-18, cell-death, *covS*, 5448, 5448AP, LEGENDplex, FLICA, inflammation, inflammasome

Introduction

Invasive infections due to the obligate human pathogen *Streptococcus pyogenes* (Group A *Streptococcus*; GAS) are characterised by unregulated inflammation and high mortality (Davies et al., 1996, Lamagni et al., 2008, Nelson et al., 2016, O'Grady et al., 2007, O'Loughlin et al., 2007, Svensson et al., 2000). The highly virulent GAS M1T1 clone 5448 is well studied (Aziz and Kotb, 2008, Tart et al., 2007, Walker et al., 2007). The propensity of M1T1 GAS to cause invasive infections is due, in part, to the increased frequency of spontaneous mutations in the two-component control of virulence regulatory system (covRS) (Walker et al., 2007), resulting in differential expression of multiple virulence factors, many of which are implicated in immune defence (Kilsgård et al., 2016, Sumby et al., 2005, Sumby et al., 2006, Walker et al., 2007). Compelling evidence describes the resistance of *covS* mutant GAS (mutation to the sensor protein of covRS) to killing by human neutrophils (polymorphonuclear leukocytes, PMNs) (Ato et al., 2008, Maamary et al., 2010, Walker et al., 2007). 5448AP (animal passaged) is one M1T1 *covS* mutant strain that shows resistance to killing by human neutrophils, has increased bacterial dissemination and results in decreased survival in mouse models of infection (Fiebig et al., 2015, Maamary et al., 2010, Walker et al., 2007). Due to these characteristics, 5448AP can be used as a

48 model strain to explore *covS* induced hypervirulence and the host response to invasive GAS
49 infection.

50 Neutrophils are the primary innate immune cell-type that defend against bacterial pathogens,
51 with their presence contributing to the overarching inflammatory response (Kobayashi et al.,
52 2018). Proteins of neutrophil origin are highly abundant at sites of invasive GAS infection
53 (Edwards et al., 2018). The neutrophil life cycle is tightly regulated to avoid the release of
54 cytotoxic contents that can damage surrounding tissue and contribute further to inflammation
55 (Epstein and Weiss, 1989, Faurschou and Borregaard, 2003). Under normal conditions cytotoxic
56 reactive oxygen species (ROS) produced by neutrophils kill phagocytosed bacteria (Nguyen et al.,
57 2017). An increased production of ROS signals for the induction of the anti-inflammatory cell-
58 death pathway apoptosis (Lundqvist-Gustafsson and Bengtsson, 1999). During apoptosis,
59 neutrophils are carefully decommissioned, ensuring no unregulated release of material, then
60 cleared by a secondary phagocyte, macrophages, through a process known as efferocytosis
61 (Bratton and Henson, 2011). The cleavage of caspase-3 to the p17 form denotes the execution of
62 apoptosis (Nicholson et al., 1995). Increased neutrophil apoptosis is described during GAS
63 infection (Kobayashi et al., 2003). Pro-inflammatory neutrophil death has also been reported
64 during GAS infection (Tsatsaronis et al., 2015). One form of pro-inflammatory death is pyroptosis,
65 involving the formation of an inflammasome and subsequent caspase-1 or caspase-4 activation,
66 culminating in cell-lysis (Man and Kanneganti, 2016, Sollberger et al., 2012). Deregulation of (or
67 excessive) pro-inflammatory neutrophil-death may therefore contribute further to inflammatory
68 pathology, as demonstrated during infection with other pathogens, including *Pseudomonas*
69 *aeruginosa* (Ryu et al., 2017) and *Staphylococcus aureus* (Ghimire et al., 2018, Greenlee-Wacker
70 et al., 2017, Ryu et al., 2017). Inflammation is also heavily influenced by cell cytokine production,
71 where increased release can invoke neutrophil dysfunction, affecting neutrophil survival,
72 antibacterial function or even migration (Brown et al., 2006, Kipnis, 2013, Kovach and Standiford,
73 2012, Norrby-Teglund et al., 2000). Previous work outlines how GAS take advantage of
74 inadequate or exacerbated immune responses and focus upon the bacterial mechanisms involved

75 (Cole et al., 2011). Although models to investigate leukocyte inflammasome activation have been
76 proposed (Tran et al., 2019), a limited number of studies have investigated the neutrophil
77 response to GAS specifically (Kobayashi et al., 2003). Here, using an *in vitro* model, we temporally
78 describe the effect two M1T1 GAS strains have upon human neutrophil death, signalling and
79 inflammatory profile. We further characterise this interaction in murine neutrophils, using an *in*
80 *vivo* model of intradermal invasive GAS infection. Additionally, we identify differences in the
81 neutrophil response to GAS due to *covS* mutation. We hypothesise that changes to neutrophil
82 function by GAS can promote invasive GAS infection by exacerbating the inflammatory response,
83 decreasing antibacterial capacity and inducing inflammatory neutrophil death.

84 **Results**

85 **GAS persistence and proliferation occurs during a dampened neutrophil ROS response**

86 Neutrophil phagocytic ability is a predominant and well-established mechanism of immune
87 defence. Both GAS strains 5448 and 5448AP rapidly associated with human neutrophils, with
88 near maximal association observed within 30 min (Figures 1A and S1A-C). Higher percentages of
89 neutrophils were associated with 5448 compared to 5448AP (Figure 1A). 5448 and 5448AP also
90 induced ROS production in neutrophils, with less ROS produced by neutrophils incubated in the
91 presence and absence of 5448AP compared to those incubated with 5448 (Figure 1B). As such,
92 the rate of neutrophil ROS production was significantly increased compared to the neutrophil
93 only control during 5448, but not 5448AP, infection ($p<0.01$, Figure S1D), suggesting dampened
94 antibacterial function in neutrophils in response to 5448AP. This difference in GAS-induced ROS
95 production inversely corresponded to GAS proliferation in the presence of neutrophils, with high
96 numbers of 5448AP observed compared to 5448 over 180 min (Figure 1C). Differential GAS
97 proliferation required viable neutrophils, as 5448 and 5448AP proliferation in the presence of
98 neutrophil lysates was reduced and similar for both strains over 180 min (Figure 1D). Finally,
99 incubation of neutrophils with the phagocytosis inhibitor cytochalasin D significantly increased
100 5448, but not 5448AP, survival ($p<0.001$, Figure S1E), indicating that 5448 killing is

101 predominantly mediated via a phagocytic-related pathway. Collectively, these data indicate that
102 compared to 5448, 5448AP associates less readily with human neutrophils leading to reduced
103 ROS production and increased survival of this strain.

104 **Figure 1. GAS persistence and proliferation occurs during a dampened neutrophil ROS**
105 **response.** (A) Association of fluorescent GAS strains with human neutrophils (PMNs, n=6
106 donors), analysed via flow cytometry (Figure S1A-B). (B) Infection of human neutrophils with
107 GAS invokes ROS production. Representative of triplicate measurements from three separate
108 experiments (n=3 donors), shown as mean change in fluorescence units over time ($\Delta F.min^{-1}$). GAS

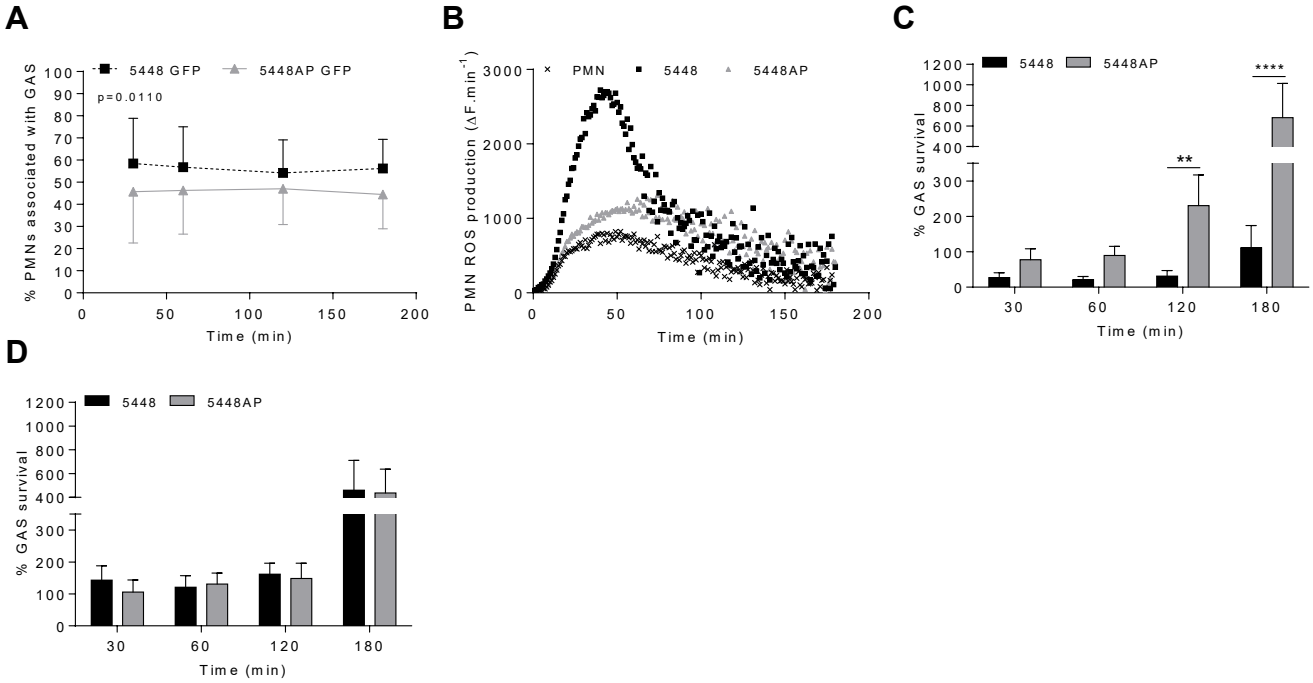

109 strains were incubated in the presence of (C) human neutrophils (n=8 donors) or (D) lysed
110 human neutrophils (n=4 donors) over 180 min with surviving bacterial concentration
111 determined as percentage over inoculum. Results are the pooled means±SD (of triplicate
112 measurements for panels C and D). **p<0.01 and ****p<0.0001.

113 **Neutrophil death is delayed during infection with *covS* GAS**

114 GAS can induce death of human neutrophils (Kobayashi et al., 2003, Tsatsaronis et al., 2015),
115 however the mechanism remains poorly described. Phosphatidylserine (PS) exposure is a

116 hallmark of the induction of multiple death pathways including apoptosis and pyroptosis (Man
117 and Kanneganti, 2016, Wang et al., 2013). Human neutrophils were incubated with 5448, 5448AP
118 or in the absence of GAS then the binding of annexin-V (AV), as a measure of PS exposure, and the
119 binding of Zombie Fixable Viability Kit (Z), as a measure of membrane integrity, were analysed
120 by flow cytometry (Figure 2). Cells were defined as viable (AV^-Z^-), PS exposed (AV^+Z^-) or dead
121 (AV^+Z^+) (Figure 2C). Neutrophils incubated without GAS remained viable over 180 min (Figure
122 2D), with 13% exposing PS (Figure 2E) and 3% dead after this time (Figure 2F). In contrast,
123 incubation of neutrophils with either 5448 or 5448AP resulted in increased PS exposure and cell-
124 death over 180 min, with significantly more cell-death during 5448 infection compared to
125 5448AP infection at 30 and 60 min ($p<0.05$, Figure 2F). Delay in the initial induction of death in
126 response to 5448AP suggests extended neutrophil viability during the early stages of infection
127 (30-60 min).

128 **GAS infection activates caspase-1 in neutrophils but reduced apoptosis occurs in response**
129 **to *covS* GAS**

130 The above data (Figure 2) suggests that both GAS strains induce rapid neutrophil death. To
131 explore the mechanism of GAS-induced neutrophil death and whether this differs between GAS
132 strains, human neutrophil lysates were separated by SDS-PAGE and screened for the abundance
133 of active caspase-3, caspase-1 and caspase-4 via immunoblotting and quantified using
134 densitometry (Figures 3A and S2A-D). Cleavage of executioner caspase-3 to p17 is a definitive
135 hallmark of apoptosis induction (Nicholson et al., 1995). Conversely, caspase-1 and caspase-4
136 activity can indicate inflammasome activation, which in turn can cleave downstream effectors of
137 pyroptosis (Man and Kanneganti, 2016, Sollberger et al., 2012). Moreover, a recent report has
138 identified the caspase-1 p46 molecule as the principal active species during inflammasome
139 activation in the cell (Boucher et al., 2018). Neutrophils incubated in the absence of GAS showed
140 limited evidence of caspase-3 cleavage to p17 (Figures 3A and S2A), while levels of caspase-1
141 reduced over 180 min (Figures 3A and S2B-C). Infection of neutrophils with 5448 significantly

142 increased the presence of caspase-3 p17 at 180 min ($p>0.0001$) compared to both 5448AP-
143 infected and uninfected neutrophils (Figures 3A and S2A). In contrast, incubation of neutrophils
144 with either GAS strain caused an upregulation of caspase-1 (Figures 3A and S2B-C). Compared to
145 uninfected neutrophils, 5448 infection significantly increased pro-caspase-1 (50kDa) at 30 min,
146 60 min ($p<0.05$) and 180 min ($p<0.01$), whilst 5448AP infection only significantly increased pro-
147 caspase-1 at 180 min ($p<0.001$, Figures 3A and S2B). Further, 5448 and 5448AP infected
148 neutrophils sustain p46 expression over 180 min, though this difference was not statistically
149 significant (Figure 3A and S2C). Significant differences were not seen in the expression of
150 caspase-1 between 5448 and 5448AP infected neutrophils. Similar to caspase-1, the abundance
151 of full-length caspase-4 in neutrophils incubated in the absence of GAS declined over time
152 (Figures 3A and S2D). In contrast, 5448 infection increased caspase-4 expression at 30 ($p<0.01$),
153 60 ($p<0.001$) and 180 min compared to uninfected neutrophils ($p<0.0001$, Figures 2A and S2D).
154 5448AP infection however, only increased caspase-4 expression at 180 min ($p<0.01$, Figures 3A
155 and S2D).

156 These above data suggest both GAS strains induce pyroptosis in neutrophils, but the response to
157 5448AP is delayed. Therefore, to explore this possibility further, human neutrophils were
158 incubated with 5448, 5448AP or in the absence of GAS and caspase-1 activity assessed using a
159 fluorogenic flow cytometric caspase-1 assay (Figures 3B and S3A-C). 5448 infected neutrophils
160 showed increased active caspase-1 at 60 min and 180 min ($p<0.05$), whilst 5448AP infection
161 increased caspase-1 at 180 min ($p<0.05$) compared to uninfected neutrophils (Figure 3B). No
162 significant differences were observed between strains although caspase-1 activity was slightly
163 reduced during 5448AP infection compared to 5448 (Figure 3B), similar to the immunoblot data
164 for caspase-1 p46 (Figures 3A and S2C). Thus, GAS infection of human neutrophils corresponds

165 to increased caspase-1 activity and caspase-4 expression, consistent with inflammasome
166 activation and pyroptosis.

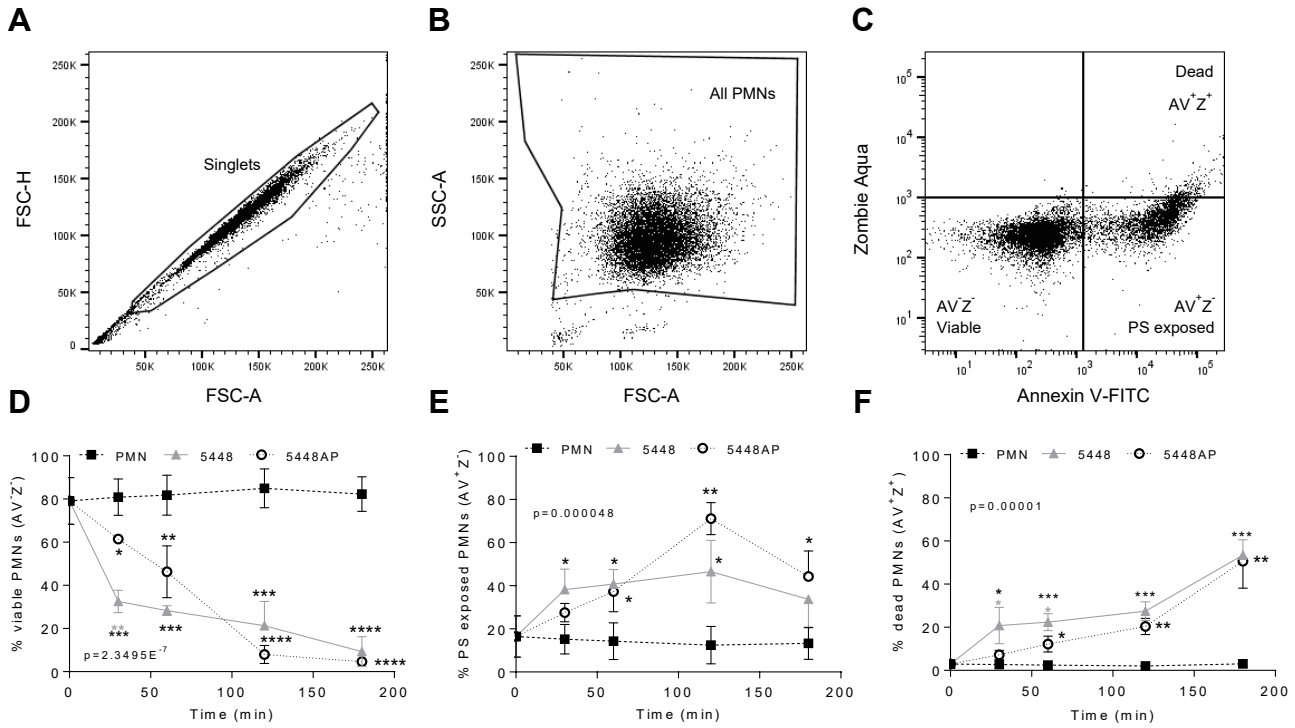

167 **Figure 2. GAS induced neutrophil death is delayed during infection with *covS* mutant.**
168 Human neutrophils (PMNs) were stained with Annexin V-FITC and Zombie Aqua Fixable Viability
169 Kit via flow cytometry and initially gated upon (A) 'Singlets' (FSC-A vs. FSC-H, 10,000 events
170 collected). 'All PMNs' (live and dead) were selected using (B) a gate excluding GAS. Cells were
171 then compared for fluorescence of (C) annexin V-FITC/phosphatidylserine (PS) binding against
172 Zombie live/dead viability dye. Purified PMNs were sampled over 180 min to measure (D) 'Viable'
173 (AV^-Z^-), (E) 'PS exposed' (AV^+Z^-), and (F) 'Dead' (AV^+Z^+), neutrophils during GAS infection (n=3
174 donors). Results are pooled means±SD . *p<0.05, **p<0.01, ***p<0.001 and ****p<0.0001, with
175 black asterisks denoting significance from control and grey asterisks between 5448 and 5448AP.

176 **Proinflammatory cytokines IL-1β and TNF-α are released by neutrophils in response to**
177 **GAS infection**

178 The release of the inflammatory cytokine IL-1β occurs due to caspase-1 activation and is
179 associated with the induction of pyroptosis (Broz et al., 2010). Uncoordinated release of various
180 inflammatory cytokines can exacerbate infection (Tecchio et al., 2014). During GAS infection,
181 disease severity is negatively correlated to cytokine concentration (Norrby-Teglund et al., 2000).
182 Therefore, human neutrophils were incubated with 5448, 5448AP or in the absence of GAS and
183 supernatants assessed for cytokines using a flow cytometric bead assay. Neutrophils incubated
184 in the absence of GAS failed to release IL-1β (Figure 3C) and TNF-α (Figure 3D) despite releasing
185 increasing amounts of IL-8 over 360 min (Figure 3E). Incubation with GAS induced IL-1β release
186 from neutrophils at 180 min and 360 min, with significantly greater release during 5448AP
187 infection compared to 5448 at 180 and 360 min ($p<0.05$, $p<0.0001$, Figure 3C). Incubation with
188 GAS also induced significant release of TNF-α from neutrophils at 180 min ($p<0.001$) and 360 min
189 ($p<0.0001$), with significantly greater release during 5448 infection compared to 5448AP at 360
190 min ($p<0.0001$, Figure 3D). 5448 induced significant release of IL-8 compared to uninfected from
191 neutrophils at 60 min and 180 min ($p<0.05$), with significantly greater release than 5448AP at 60
192 min ($p<0.05$, Figure 3E). Neutrophils released minimal amounts of IL-18 over 360 min, and
193 infection with both 5448 or 5448AP did not change this response (Figure 3F), suggesting that
194 neutrophils have no major role in IL-18 release over 360 min *in vitro*. These data indicate that
195 both 5448 and 5448AP induce IL-1β release from human neutrophils, consistent with the
196 hypothesis that both GAS strains induce pyroptosis in these cells. Moreover, the results indicate
197 differential cytokine release from human neutrophils infected with GAS, with 5448AP inducing
198 greater IL-1β release and 5448 inducing greater TNF-α and IL-8 release.

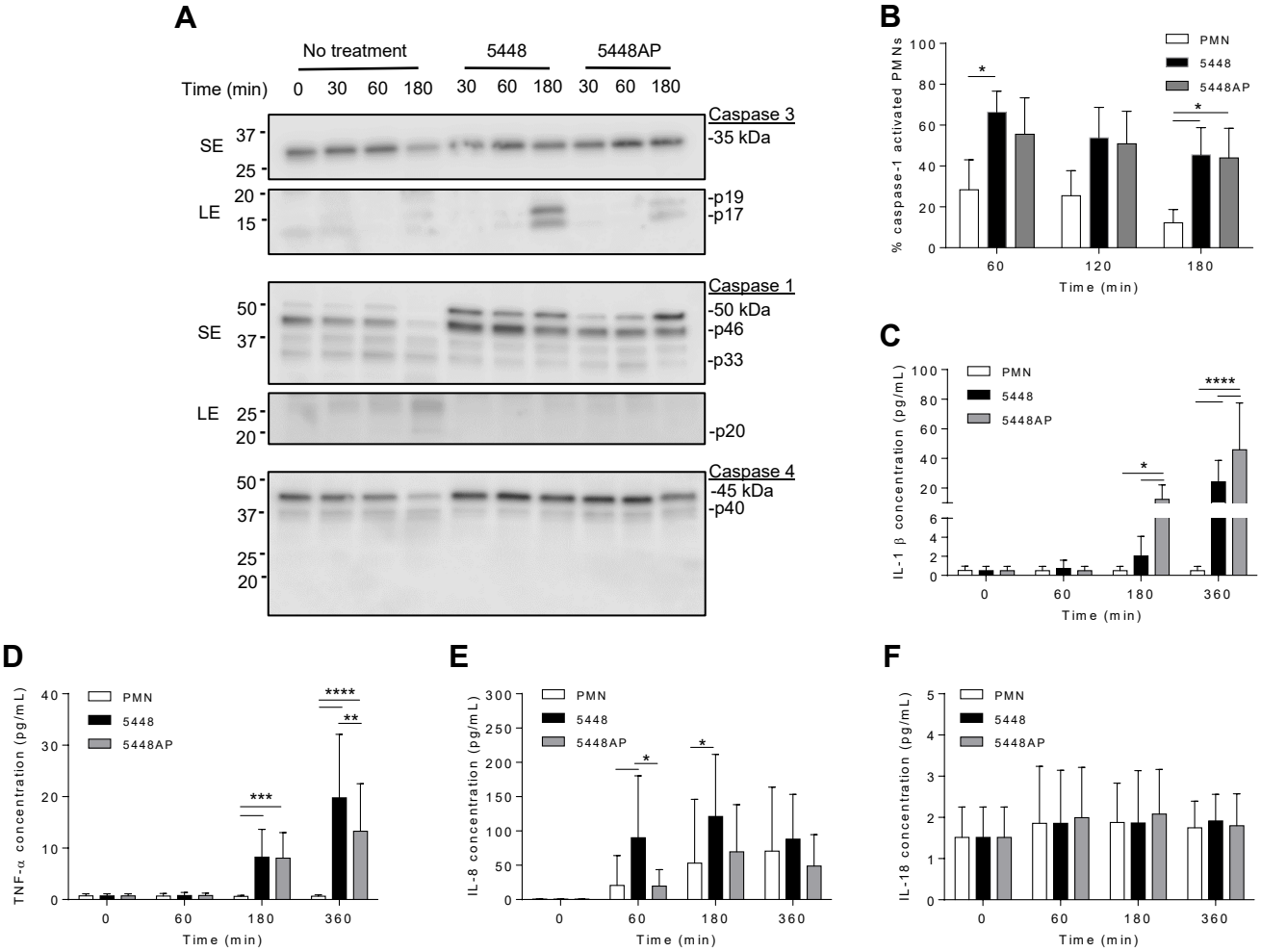

Figure 3. GAS infection activates caspase-1 in human neutrophils and induces proinflammatory cytokine IL-1β and TNF-α release. (A) Human neutrophil (PMN) lysates were prepared at 30, 60 and 180 min during GAS infection and compared to uninfected neutrophils (0, 30, 60, 180 min) via immunoblotting of caspase-3, caspase-1 and caspase-4. Images shown are from a single donor and are representative of triplicate experiments using different donors. Immunoblot bands were quantified (ImageJ) and normalised over total protein (Figure S2). SE=short exposure, LE=long exposure. (B) Caspase-1 activation in human neutrophils due to GAS infection was confirmed via flow cytometry using FLICA (FAM-YVAD-FMK) (n=3 donors). Flow cytometry gating strategy used singlets/PMNs (figure S3A) and FAM-FLICA fluorescence (Figure S3B). The release of cytokines from neutrophils during GAS infection was measured using the LEGENDplex™ human inflammation cytometric bead assay over 360 min. Neutrophils differentially released (C) IL-1β, (D) TNF-α, (E) IL-8 and (F) IL-18 in response to GAS

211 infection (duplicate measurements, n=6 donors). (B-F) Results are the pooled means±SD.
212 *p<0.05, **p<0.01, ***p<0.001 and ****p<0.0001.

213 **GAS infection may cause neutrophil dysfunction**

214 Neutrophil adhesion and activation are central to the innate immune response, with CD11b (Mac-
215 1) and CD66b (CEACAM8) playing key respective roles (Arnaout, 1990, Power et al., 2001, Skubitz
216 et al., 1996). CD16 (FcγRIII) facilitates opsonisation of pathogens and is down-regulated during
217 apoptosis (Dransfield et al., 1994, Fossati et al., 2002), whilst down-regulation of CD31 (PECAM-
218 1) facilitates clearance of apoptotic neutrophils and the resolution of inflammation (Brown et al.,
219 2002, Kurosaka et al., 2003). Therefore, to further explore the impact of GAS on neutrophil
220 function, human neutrophils were incubated with 5448, 5448AP or in the absence of GAS and the
221 expression of cell-surface CD11b, CD66b, CD16 and CD31 was assessed using flow cytometry
222 (Figure 4A-F). In the absence of GAS, neutrophils displayed minor increases in CD11b expression
223 over time, while incubation with GAS resulted in minor decreases over time, with 5448 inducing
224 a greater loss of CD11b than 5448AP, though these differences were not statistically significant
225 (p=0.289, Figure 4C). Neutrophils incubated in the absence of GAS revealed minor increases in
226 cell-surface CD66b expression over time (Figure 4D). Incubation with GAS further increased
227 expression of CD66b, with 5448 inducing a slightly greater increase than 5448AP, though these
228 differences were not statistically significant (p=0.162, Figure 4D). Incubation of neutrophils in
229 the absence of GAS resulted in a steady decline in CD16 expression over time, a loss significantly
230 increased by co-incubation with either GAS strain 180 min post-infection (p<0.0001, Figure 4E).
231 Notably, incubation of neutrophils with 5448 induced a significantly greater loss of CD16
232 expression than 5448AP incubation at all earlier time points (Figure 4E). Similar to CD16,
233 incubation of neutrophils in the absence of GAS resulted in a steady decline in CD31 expression
234 over time, a loss significantly increased by co-incubation with either GAS strain 180 min post-
235 infection (p<0.0001, Figure 4F). Moreover, incubation of neutrophils with 5448 induced a
236 significantly greater loss of CD31 expression than 5448AP incubation at earlier time points.

237 Collectively, these data indicate that GAS has minimal impact upon human neutrophil CD11b and
238 CD66b, but increases the loss of CD16 and CD31 expression, which may impact opsonisation of
239 GAS and subsequent efferocytosis of neutrophils by macrophages, during infection.

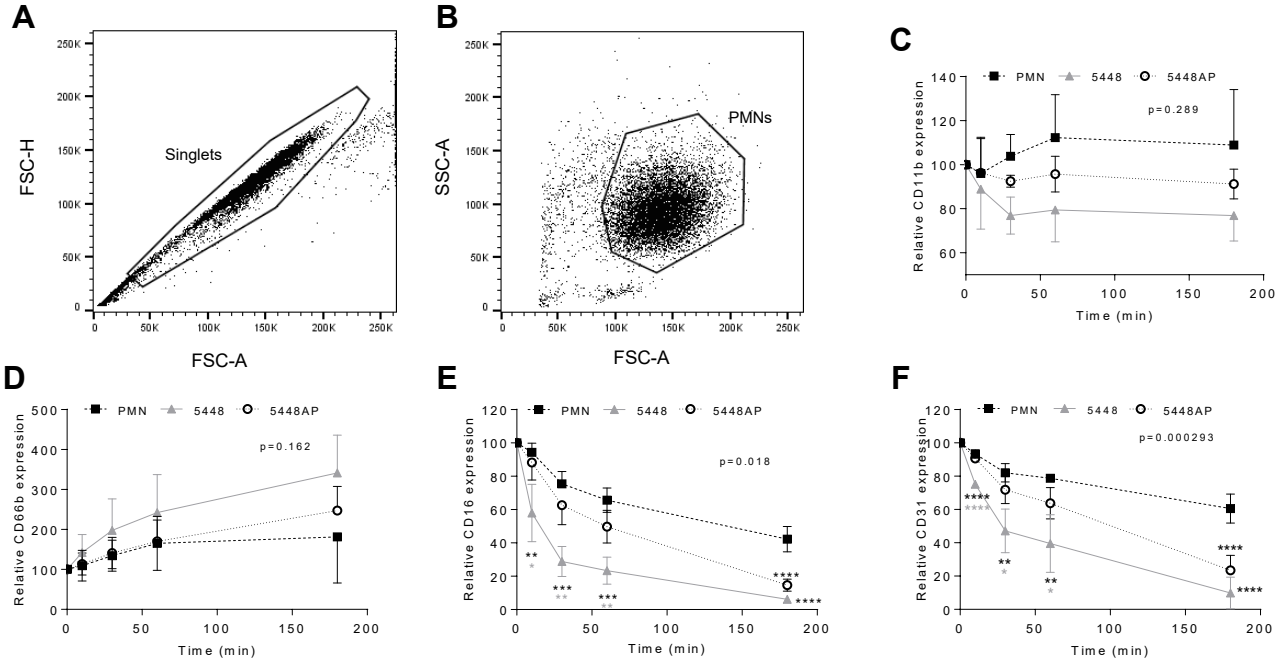

240 **Figure 4. GAS infection changes neutrophil functionality.** Human neutrophils (PMNs) were
241 analysed using flow cytometry, sequentially gated upon (A) 'Singlets' (FSC-A vs. FSC-H, 10,000
242 events collected) then (B) viable 'PMNs' (FSC-A vs. FSC-H). Purified neutrophils infected with GAS
243 were sampled over 180 min for the cell-surface expression of (C) CD11b-FITC (n=4 donors), (D)
244 CD66b-PerCP/Cy5.5 (n=5 donors), (E) CD16-FITC (n=4 donors) and (F) CD31-PE/Cy7 (n=4
245 donors). Results are the pooled means±SD. *p<0.05, **p<0.01, ***p<0.001 and ****p<0.0001, with
246 black asterisks denoting significance from control and grey asterisks between 5448 and 5448AP.

247 **GAS infection activates caspase-1 in neutrophils *in vivo***

248 The above data indicate that GAS influences human neutrophils *in vitro.* To explore if GAS may
249 alter neutrophils *in vivo*, we assessed the neutrophil response in a mouse model of GAS infection
250 (Ly et al., 2014, Maamary et al., 2010, Tsatsaronis et al., 2014). C57BL/6J mice were injected
251 intradermally with 5448, 5448AP or saline and euthanised at 6 or 24 hours post infection, with
252 neutrophil populations ($CD45^+/CD11b^+/Ly\text{-}6G^+$) and caspase-1 activation characterised by flow

253 cytometry (Figures 5A-B and S4A-F). Infection of mice with either GAS strain increased
254 neutrophil populations at sites of injection, however only 5448AP infection resulted in
255 significantly greater neutrophil numbers than the saline control at 24 h ($p<0.01$, Figure 5A). The
256 percentage of circulating neutrophils in the blood was also significantly increased due to 5448
257 ($p<0.05$) and 5448AP ($p<0.01$) infection at 6 h, however returned to baseline after 24 h (Figure
258 S4G), indicating the importance of neutrophils during the early stages of infection. Murine
259 neutrophils lavaged from sites of saline injection had low amounts of active caspase-1 (Figure
260 5B). Infection with 5448AP, but not 5448, significantly increased caspase-1 activation at 6 h
261 ($p<0.05$), while both strains increased caspase-1 activation at 24 h ($p<0.01$, Figure 5B). Cytokines
262 were assessed in murine serum using a flow cytometric bead assay. IL-1β concentrations
263 remained low for saline control and 5448 infected mice but were significantly increased at 24 h
264 during 5448AP infection ($p<0.0001$, Figure 5C).

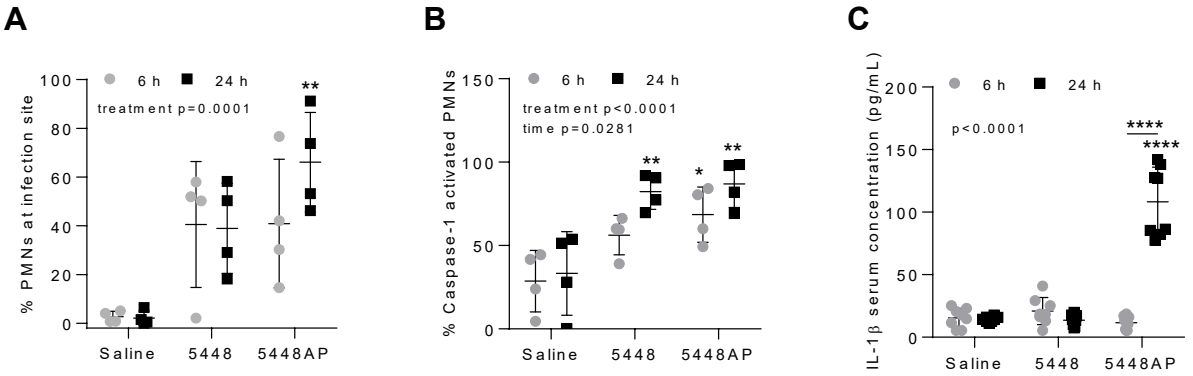

265 **Figure 5. GAS infection *in vivo* activates caspase-1 in murine neutrophils.** (A) Percentage of
266 $CD45^+$ cells lavaged from site of injection characterised as neutrophils (PMNs, $CD11b^+$/Ly-$6G^+$)
267 by flow cytometry (Figure S4A-E). (B) Caspase-1 activation in neutrophils at site of GAS infection
268 was confirmed via flow cytometry using FLICA 660 (660-YVAD-FMK, Figure S4F). Each data point
269 represents the results from a single mouse where n=4. (C) The release of IL-1β in mouse serum
270 during GAS infection was measured using the LEGENDplex™ mouse inflammation cytometric
271 bead assay at 6 and 24 h post infection where duplicate measurements are shown and n=4.
272 Results are the mean±SD. **$p<0.01$, ***$p<0.001$ and ****$p<0.0001$ where significance is denoted
273 from control or as indicated by a line.

274 **Discussion**

275 Here we have mapped the human neutrophil response to GAS, addressing cell-death, signalling
276 and the inflammatory profile during the early stages of M1T1 (5448 and 5448AP) infection. For
277 the first time, we describe an inflammatory neutrophil phenotype, as evidenced by caspase-1
278 activation, that may promote inflammation and exacerbate GAS disease. Most notably, changes to
279 the expression of cell-surface proteins CD16 and CD31 may impede the removal of bacteria and
280 clearance of neutrophils at sites of infection, hindering the resolution of inflammation. Further,
281 we elucidate differences between 5448 and 5448AP that aid in understanding the survival and
282 proliferation of GAS harbouring *covS* mutations in the presence of human neutrophils.

283 The temporal expression of neutrophil cell surface markers has not previously been investigated
284 in the context of GAS infection. Our data show that significant reductions to both CD16 and CD31
285 occur in neutrophils due to GAS infection *in vitro*. CD16 functions as a receptor for opsonised
286 bacteria and immune complexes (Fossati et al., 2002), whilst the loss of CD16 has also been
287 associated with the induction of apoptosis (Dransfield et al., 1994). The induction of apoptosis
288 following bacterial phagocytosis is advantageous to the host as it promotes controlled removal of
289 bacteria and the resolution of inflammation (Kobayashi et al., 2018). We hypothesise that the
290 retention of CD16 during infection promotes a reduction in apoptosis and prolonged
291 degranulation at the site of infection. Further, CD31 expression is reduced during GAS infection,
292 facilitating the eventual removal of neutrophils from sites of infection (Kobayashi et al., 2003).
293 Parallel to CD16, CD31 is retained during 5448AP infection of neutrophils to a greater extent than
294 5448 infection. This may result in neutrophils remaining at sites of infection longer, further
295 increasing inflammation. Additionally, we report a trend towards increased cell-surface
296 expression of CD11b and CD66b during GAS infection. Migration of neutrophils to sites of
297 infection, facilitated by CD11b-mediated neutrophil adhesion (Arnaout, 1990), may therefore be
298 affected during GAS infection. Down-regulation of CD11b can prevent accumulation of
299 neutrophils at inflammatory sites (Huston et al., 2009), however retention, such as that seen

300 during 5448AP infection may contribute to prolonged inflammation. Neutrophil activation can be
301 determined through the expression of cell-surface CD66b following stimulation (Skubitz et al.,
302 1996). Reduced cell-surface CD66b expression in response to 5448AP infection may therefore
303 indicate a reduction to neutrophil function and further explain the resistance to neutrophil-
304 mediated killing. Collectively, the neutrophil response is altered and inflammation prolonged at
305 sites of *covS* mutant GAS infection.

306 Disruption of the role neutrophils play during the resolution of GAS infection and induction of
307 inflammatory death pathways has been reported previously (Kobayashi et al., 2003, Tsatsaronis
308 et al., 2015). Proinflammatory activation of the NLRP3 inflammasome in macrophages has been
309 demonstrated for M1 GAS (Valderrama et al., 2017), here we provide the first evidence that GAS
310 activates caspase-1 in human and murine neutrophils, consistent with inflammasome activation
311 and pyroptosis. Caspase-1 activation was consistent during infection with both M1T1 GAS
312 isolates, however the release of inflammatory cytokine IL-1β, a hallmark of clinical invasive
313 infection (LaRock and Nizet, 2015), was significantly increased in response to 5448AP infection
314 *in vitro* and *in vivo*. In murine bone marrow-derived dendritic cells caspase-1 activation is
315 essential for IL-1β release (Schneider et al., 2017). The activation of caspase-1 in human and
316 murine neutrophils does not correlate directly to the amount of IL-1β released, and an alternative
317 mechanism may facilitate IL-1β maturation. Type I interferons are known regulators of IL-1β in
318 GAS infected mice (Castiglia et al., 2016), where increased IL-1β release in murine serum seen in
319 this study may also be attributed to disruption of this homeostatic relationship. Increased IL-1β,
320 being a neutrophil chemoattractant, therefore may further promote inflammation at sites of
321 infection following release (Chen et al., 2007), supporting the hypothesis that *covS* mutant GAS
322 promote greater levels of inflammation during GAS infection.

323 Previous studies have characterised differences between 5448 and 5448AP, demonstrating
324 resistance to neutrophil-mediated killing *in vitro* and increased bacterial dissemination and
325 decreased survival *in vivo* following the acquisition of *covS* mutations (Fiebig et al., 2015,

326 Maamary et al., 2010, Walker et al., 2007). Here, we demonstrate that 5448AP is not only resistant
327 to neutrophil-mediated killing but proliferates in the presence of functional neutrophils. GAS
328 survival has been demonstrated intracellularly in murine neutrophils and human macrophages
329 (Medina et al., 2003a, Medina et al., 2003b, O'Neill et al., 2016) and can even be facilitated by host
330 red blood cells (Wierzbicki et al., 2019). Increased 5448AP proliferation may result from the
331 reduction in neutrophil ROS response during infection. GAS has previously been shown to display
332 resistance to ROS through numerous virulence mechanisms (Henningham et al., 2015). The
333 absence of a hostile environment may further permit bacterial replication. Additionally, the
334 increased production of ROS can induce neutrophil death via apoptosis (Geering and Simon,
335 2011). Reduced neutrophil ROS production during 5448AP infection may therefore explain the
336 reduction seen in caspase-3 activation (apoptosis). Previously it has been demonstrated that GAS
337 M1 strain MGAS5005 modulates neutrophil apoptosis (Kobayashi et al., 2003), a finding which is
338 supported by the current study.

339 Changes to the function of neutrophils during the initial innate immune response have the
340 potential to hinder mechanisms essential for the resolution of infection. Disruption to these
341 processes during GAS infection may induce this neutrophil phenotype we have described, with
342 increased inflammatory properties and potential to exacerbate infection. Caspase-1 activation
343 during GAS infection of neutrophils indicates possible inflammasome activation and death via
344 pyroptosis. Further studies should explore the precise cell death mechanism. A reduction in
345 apoptosis is evident during *covS* GAS infection, as has been reported for non-M1T1 GAS
346 (Tsatsaronis et al., 2015), whilst modulation of apoptosis has previously been implicated as a
347 factor contributing to GAS survival (Kobayashi et al., 2003). The current study aids in
348 understanding the complex host-pathogen interaction identifying host factors that may
349 contribute to severe pathology of invasive GAS infection. Future studies may be able to isolate
350 host-specific targets that could be exploited to control inflammation and tissue damage during
351 invasive GAS infection.

352 **Acknowledgements**

353 We thank Professor Marijka Batterham (University of Wollongong) for her statistical
354 consultation. We thank Associate Professor Thomas Proft (University of Auckland, New Zealand)
355 for pLZ12Km2-P23R:TA. We also thank our generous blood donors for their participation and
356 time.

357 **Author Contributions**

358 Conceptualisation, M.S.S, R.S., J.A.T., J.G.W.; Methodology, M.S.S., R.S., J.G.W., J.G., J.D.M., D.L.;
359 Investigation, J.G.W., D.L., N.J.G., H.K.N.V.; Data and figure curation, J.G.W., D.L., R.S., M.S.S.; Writing-
360 Original draft, J.G.W.; Writing-Review and editing, M.S.S., R.S., J.G.W., D.L., N.J.G., J.D.M., H.K.N.V.,
361 J.G., J.A.T.; Funding acquisition, M.S.S and D.L.; Resources, M.S.S., J.D.M.; Supervision, M.S.S., R.S.,
362 J.G.

363 **Declaration of Interests**

364 The authors declare no competing interests.

365 **STAR Methods**

366 **Ethics statement**

367 All experiments involving the use of human blood were conducted with informed consent of
368 healthy volunteers, approved and authorised by the University of Wollongong Human Research
369 Ethics Committee (Protocol HE08/250). All experiments involving the use of animals were
370 approved and authorised by the University of Wollongong Animal Ethics Committee (Protocol
371 AE18/10).

372 **Bacterial strains and culture**

373 *Escherichia coli* MC106 were grown in Luria–Bertani Broth (LB) at 37 °C with constant shaking.
374 M1T1 *S. pyogenes* invasive clinical isolate 5448 (*emm1*) and hypervirulent animal passaged

375 5448AP (containing a non-functional control of virulence regulator mutation) have been
376 described previously (Aziz et al., 2004, Chatellier et al., 2000). GAS strains were routinely cultured
377 at 37°C on horse-blood agar (Thermo Fisher) and enumerated on yeast supplemented (1% w/v)
378 Todd-Hewitt (THY, Benton Dickson) agar. Static overnight cultures were grown at 37°C in THY
379 then sub-inoculated (1:10) into fresh THY and grown to mid-logarithmic phase, antibiotics were
380 added when required (100 μg/ml ampicillin and 200 μg/ml kanamycin). Bacterial pellets were
381 washed twice with phosphate buffered saline (PBS) then resuspended at the specified
382 multiplicity of infection (MOI) and assay specific media conditions.

383 **Construction of GFP expression vector pLZ12Km2-P23R-TA:GFP for GAS**

384 In brief, stable GFP expression by GAS was created by synthesizing the ribosomal binding site
385 (RBS) and *gfp* gene from pDC*erm*-GFP (Ly et al., 2014) into the pUC57 plasmid (GenScript),
386 resulting in pUC57-RBSGFP plasmid. RBS and *gfp* from pUC57-RBSGFP were then sub-cloned
387 using NotI into the toxin–antitoxin (TA) stabilized expression plasmid pLZ12Km2-P23R:TA,
388 kindly provided by Associate Professor Thomas Proft (University of Auckland, New Zealand) (Loh
389 and Proft, 2013), to produce pLZ12Km2-P23R-TA:GFP. The resultant plasmid system utilises the
390 *Streptococcal* ω–ε–ζ TA cassette to achieve segregational plasmid stability under non-selective
391 conditions (Lioy et al., 2010).

392 Specifically, plasmids pLZ12Km2-P23R:TA and pUC57-RBSGFP (engineered with RBS and *gfp*
393 from pDC*erm*-GFP) were first transformed into chemically competent *E. coli* MC106 via
394 electroporation. The plasmids were then retrieved and purified from *E. coli* cultures using a
395 Wizard® Plus SV Minipreps DNA Purification System (Promega). The pLZ12Km2-P23R:TA
396 plasmid was digested with 20 U NotI enzyme and further treated with 5 U shrimp alkaline
397 phosphatase. The pUC57-RBSGFP plasmid was also incubated with 20 U NotI to excise the RBS
398 and *gfp* gene from pUC57-RBSGFP, and these were then ligated into digested pLZ12km2-P23R:TA
399 plasmid. The resulting plasmid, pLZ12Km2-P23R-TA:GFP, was then transformed and cloned in
400 MC106 *E. coli*, and later extracted and purified. pLZ12Km2-P23R-TA:GFP was transformed into

401 GAS using standard GAS electroporation techniques (McLaughlin and Ferretti, 1995).
402 Transformed GAS was confirmed for GFP expression via flow cytometry.

403 **Isolation of human neutrophils**

404 Venous human blood was drawn into 10 mL lithium heparin-coated Vacutainer (Benton Dickson)
405 tubes and layered over equal volumes of Polymorphprep (Axis Shield) and centrifuged as per
406 manufacturer's instructions. The resulting layer of neutrophils was isolated and erythrocytes
407 hypotonically lysed. Isotonic concentration was restored with Hank's Balanced Salt solution
408 (without Ca^{2+} or Mg^{2+}, Corning Inc.). Prior to experimentation neutrophils were resuspended at
409 specified concentrations in complete medium, Roswell Park Memorial Institute (RPMI)-1640
410 medium (Life Technologies) containing 2% heat-inactivated autologous plasma and 2 mM L-
411 glutamine (Life Technologies), unless otherwise stated. Neutrophil viability was assessed via
412 Trypan Blue (Sigma-Aldrich) staining and neutrophil purity was assessed using a Benton Dickson
413 LSR Fortessa X-20 flow cytometer via distinct forward and side scatter profiles or CD66b-
414 peridinin chlorophyll protein (PerCP)/Cy5.5 (clone G10F5, BioLegend) expression. Neutrophils
415 were maintained at room temperature throughout processing.

416 ***In vitro* infection of neutrophils with GAS**

417 Purified human neutrophils were seeded in either 96-well plates at MOI (GAS:neutrophil) 1:10
418 (survival and proliferation) or 10:1 (ROS production and cytokine release), 24-well plates at 10:1
419 (phagocytosis, Annexin-V/Viability staining, CD expression and FAM-FLICA caspase-1 activation)
420 or 6-well plates at 10:1 (immunoblotting) and incubated at 37°C in 5% CO_2.

421 **GAS survival and proliferation**

422 Human neutrophils were co-cultured with GAS or lysed via three freeze-thaw cycles prior to
423 incubation. To block phagocytosis neutrophils were preincubated with 10 μm cytochalasin D
424 (Cayman Chemicals) in complete medium at 37°C for 30 min prior to infection. At indicated time

425 points neutrophils were hypotonically lysed and surviving bacteria serially diluted before plating
426 on THY agar.

427 **GAS phagocytosis**

428 Human neutrophils were co-cultured with GAS expressing GFP for the times indicated in
429 complete medium. Cells were removed and washed twice with 10% (v/v) heat-inactivated foetal
430 bovine serum (FBS, Bovogen Biologicals) diluted in PBS, followed by data acquisition via flow
431 cytometry.

432 **ROS production**

433 ROS production was assessed as previously described (Kobayashi et al., 2003). Briefly, prior to
434 infection, human neutrophils were incubated in complete medium containing 25 μM
435 dichlorofluorescein (DCF, Molecular Probes) for 45 min at room temperature (RT). ROS
436 production was measured fluorometrically ($_{ex}$485 nm $_{em}$520 nm) using a POLARstar Omega plate
437 reader (BMG Labtech).

438 **Flow cytometry**

439 For human neutrophil in vitro assays, flow cytometry data was acquired using a BD LSR Fortessa
440 X-20 with excitation lasers; violet (405 nm), blue (488 nm), yellow/green (561 nm) and red (640
441 nm). Bandpass filters for Zombie Aqua Fixable Viability Kit (525/50), fluorescein isothiocynate
442 (FITC)/GFP/FAM FLICA (525/50), PerCP-Cy5.5 (695/40) R-phycoerythrin (PE, 586/15),
443 propidium iodide (PI, 610/20), PE-Cy7 (780/60) and allophycocyanin (APC, 670/30) were used.
444 For murine infection studies, flow cytometry data was acquired using an Invitrogen Attune NxT
445 with excitation lasers; violet (405 nm), blue (488 nm), yellow (561 nm) and red (638 nm).
446 Bandpass filters VL1 (440/50), VL2 (512/25), BL1 (530/30), YL1 (585/16), YL3 (695/40) and
447 RL2 (720/30) were used. Data was analysed using FlowJo software V10.6.1 (TreeStar Inc.).

448 **Annexin-V/viability staining**

449 To assess cell viability human neutrophils at indicated times were washed with PBS and
450 incubated with Zombie Aqua Fixable Viability Kit (BioLegend) for 15 min at RT. Cells were
451 washed again once with PBS, then 10% (v/v) FBS in PBS and stained with Annexin-V-FTIC
452 (BioLegend) for 15 min at RT. Cells were analysed immediately via flow cytometry.

453 **Immunoblotting and antibodies**

454 Following co-culture in the presence or absence of GAS, human neutrophil lysates were prepared
455 in RIPA buffer (150 mM NaCl, 5 mM EDTA, 50 mM Tris, 1.0% (v/v) Triton X-100, 0.1% (w/v) SDS,
456 0.5% (w/v) sodium deoxycholate, 2x cOmplete protease inhibitor cocktail (Roche), 1 mM
457 phenylmethylsulphonyl fluoride, 5 mM sodium pyrophosphate, 5 mM sodium molybdate and 5
458 mM β-glycerophosphate) following co-culture in the presence or absence of GAS and incubated
459 for 30 min on ice with intermittent vortexing. Soluble fractions were separated via centrifugation
460 at 4°C, snap frozen in liquid N_2 and stored at -80°C. Protein concentrations were determined by
461 comparison to bovine serum albumin standards using the DC Protein Assay (Bio-Rad) and
462 absorbance (A_{750nm}) measured using a POLARstar Omega plate reader. Neutrophil lysates (20 µg)
463 were separated on 4-20% TGX Stain-Free protein gels (Bio-Rad) as per the manufacturer's
464 running conditions then activated for 5 min under UV to determine total protein (Bio-Rad
465 ChemiDoc XR, Image Lab Software). Proteins were transferred to PVDF membranes (Bio-Rad),
466 blocked, then incubated overnight at 4°C with caspase-1 polyclonal (1:1000, #2225), caspase-3
467 polyclonal (1:1000, #9662), caspase-4 polyclonal (1:1000, #4450) or caspase-8 monoclonal
468 (1:1000, #4790) antibodies (Cell Signalling Technology). PVDF membranes were washed thrice
469 between incubations for 5 min with tris-buffered saline containing 0.1% (v/v) Tween 20. PVDF
470 membranes were incubated with horseradish peroxidase-conjugated goatαrabbit IgG (1:5000,
471 Invitrogen) for 1 h at RT and detected using Clarity or Clarity Max Western ECL Blotting Substrate
472 (Bio-Rad) and imaged (Amersham AI600). Bands were quantified using ImageJ software
473 (National Institutes of Health) as area under the peak and normalised over UV determined total
474 protein.

475 **FAM-FLICA caspase-1 activation**

476 Caspase-1 activation was measured using FAM-FLICA Caspase-1 assay kit (ImmunoChemistry
477 Technologies) as per the manufacturer's instructions. In brief, following co-culture of human
478 neutrophils with GAS, cells were removed and incubated in serum free medium (RPMI-1640)
479 containing 1 x FAM-YVAD-FMK for 60 min at 37°C. Cells were then analysed for caspase-1
480 activation via flow cytometry.

481 **Cytometric cytokine bead assay**

482 Human neutrophil supernatants were at indicated times during GAS infection, snap frozen with
483 liquid N_2 and stored at -80°C for a period no longer than 5 days. Neutrophils were assessed for
484 the release of cytokines IL-1β, IL-8, IL-18 and TNF-α using the LEGENDplex™ human
485 inflammation panel bead-based immunoassay (BioLegend) and flow cytometry as per
486 manufacturer's instructions. In brief, samples and standards were incubated with beads and
487 detection antibodies for 120 min at room temperature, with shaking (600 rpm) protected from
488 light. PE-conjugated streptavidin was then added and incubated for a further 30 min at room
489 temperature, with shaking (600 rpm) protected from light. Beads were washed twice with
490 LEGENDplex™ wash buffer and data collected via flow cytometry. Beads were initially gated upon
491 FSC-A and SSC-A (A and B populations). Cytokines have signature APC fluorescence with
492 quantitative expression determined using PE fluorescence in comparison to cytokine standards.
493 Data was analysed using the LEGENDplex™ software V8.0 (VigeneTech Inc.).

494 **Cluster of differentiation expression**

495 Human neutrophil cell surface CD expression was assessed during GAS infection. Neutrophils at
496 indicated times were washed with PBS then routinely incubated with Zombie Aqua Fixable
497 Viability Kit for 15 min at RT. Cells were washed once again in PBS, followed by 10% (v/v) FBS in
498 PBS. Neutrophils were stained with fluorochrome-conjugated antibodies CD11b-FITC (Clone
499 ICRF44), CD31-PE/Cy7 (Clone WM59), or CD66b-PerCP/Cy5.5 (Clone G10F5) (BioLegend) and

500 CD16-FITC (Clone 3G8, Benton Dickson) for 15 min at RT. Neutrophils were washed with 10%
501 (v/v) FBS in PBS then analysed via flow cytometry.

502 **Murine intradermal GAS infection model**

503 Intradermal GAS challenge of C57BL/6J mice has been described previously (Ly et al., 2014,
504 Maamary et al., 2010, Tsatsaronis et al., 2014). In brief, equal numbers of 6-8 week old male and
505 female C57BL/6J mice (Australian BioResources) were anesthetised via isoflurane inhalation,
506 followed by two intradermal injections into shaved left and right flanks with either 1 x 10^8 CFU
507 of mid-logarithmic GAS or 100 µL sterile 0.7% saline. Mice were euthanised via slow-fill CO_2
508 asphyxiation at 6 or 24 h post-infection. Blood collected via cardiac puncture was separated into
509 two aliquots for serum and flow cytometric analysis. Serum was collected by clotting for 1 h at RT
510 then placed on ice until centrifugation at 1200 x *g* for 10 min at 4°C, then immediately stored at -
511 80°C until use. Remaining blood samples were mixed with 20 µL 0.5% sodium citrate (w/v) per
512 mL of blood and placed on ice. Equal volume of PBS was added to the blood sample and
513 centrifuged at 350 x *g* for 5 min. For erythrocyte lysis, samples were incubated with 1 mL of
514 ammonium-chloride-potassium lysing buffer (150 mM NH_4Cl, 1 mM $KHCO_3$, 0.1 mM Na_2CO_3, pH
515 7.3) for 5 min with gentle agitation and centrifuged at 350 x *g* for 5 min. This process was repeated
516 and cells were then washed with PBS and resuspended in 500 µL PBS and placed on ice.
517 Additionally, sites of infection were lavaged with 1 mL of sterile 0.7% saline, and fluid collected
518 from both right and left flanks was pooled to increase cell numbers. Pooled samples were kept
519 cold until centrifugation at 350 x G for 5 min, resuspended in 500 uL of PBS and placed on ice.
520 Both blood and lavage fluid samples were analysed via flow cytometry.

521 **Flow cytometric analysis of murine cells**

522 Cell viability was assessed as described above. To assess caspase-1 activation and CD expression,
523 cells were initially washed with 1 mL of PBS, followed by 1 mL of 10% (v/v) FBS in PBS. Cells
524 were then centrifuged and simultaneously stained with 1 x 660-YVAD-FMK (FLICA 660 Caspase-

525 1 assay kit, ImmunoChemistry Technologies) for caspase-1 activation and with fluorochrome-
526 conjugated antibodies CD45-BV421 (clone 30-F11), CD11b-PE/Cy5 (clone M1-70) and Ly-6G-PE
527 (clone 1A8) (Biolegend) in RPMI 1640 media for 30 min at RT . Cells were washed with 10% (v/v)
528 FBS in PBSand analysed via flow cytometry.

529 **Murine serum IL-1β concentration**

530 IL-1β release was measured in murine serum using the LEGENDplex™ mouse inflammation panel
531 bead-based immunoassay (BioLegend) and flow cytometry as described above except shaking
532 was performed at 800 rpm.

533 **Statistical analyses**

534 Graphs were created using Prism 6 (GraphPad Software Inc.) and statistical analysis was
535 performed using Prism 6 and IBM SPSS Statistics 25 (IBM® corporation). Data was analysed
536 using one-way and two-way ANOVA to determine significant differences and adjusted using
537 Tukey HSD corrections or as stated otherwise. To account for the nested nature of the human
538 neutrophil Annexin-V/Zombie and CD data with repeated measures over time in the same donor,
539 a linear mixed model was used to determine significant interaction between treatment and time.
540 Post-hoc tests were performed by multiple one-way ANOVA at each time point where multiple
541 comparisons were adjusted using Tukey HSD corrections. *In vivo* data was analysed by two-way
542 ANOVA where differences are shown between treatment and time, also using Tukey HSD
543 corrections. Values presented for 'p' represent interaction (treatment*time) unless otherwise
544 stated. * $p<0.05$; ** $p<0.01$; *** $p<0.001$; **** $p<0.0001$.

545

546 **Supplemental Information**

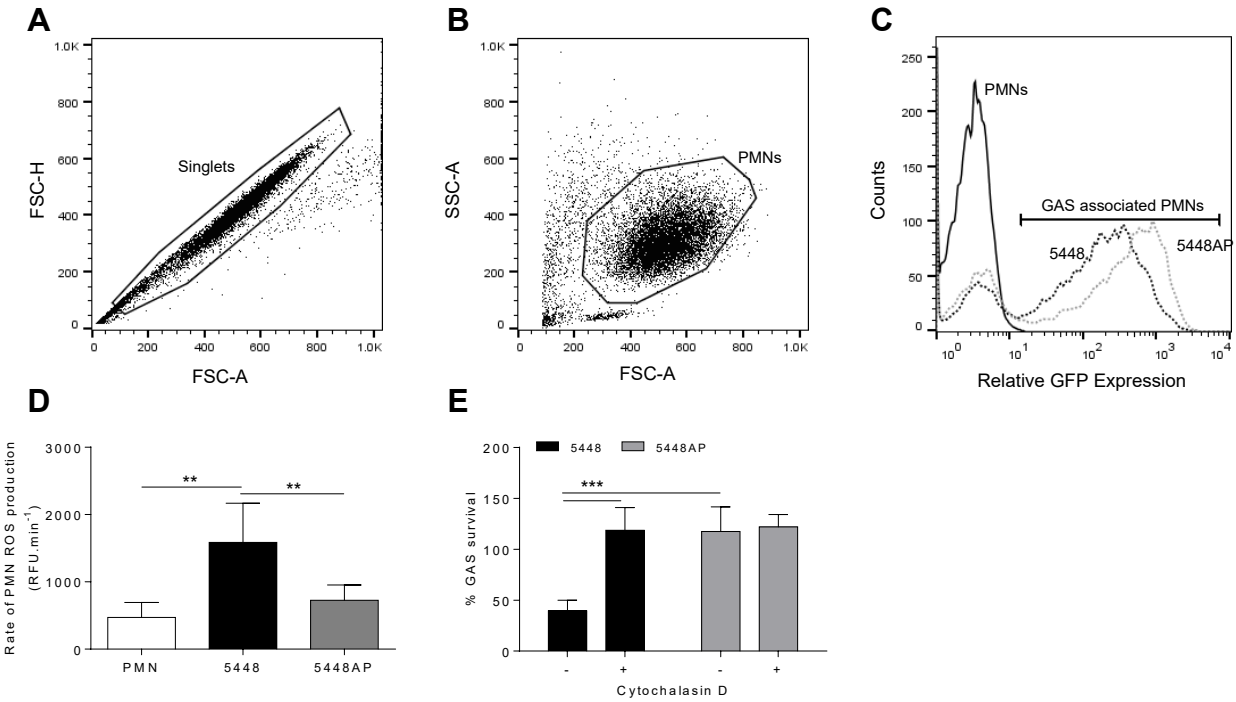

547 **Supplementary figure 1. The association of fluorescent GAS (GFP) to human neutrophils**
548 **determined via flow cytometry.** (A) Primary neutrophil (PMN) 'Singlets' cell selection (FSC-A
549 vs. FSC-H) and (B) viable 'PMNs' discrimination (FSC-A vs. SSC-A). (C) Representative histogram
550 showing relative fluorescence (GFP) of GAS infected neutrophils and gating for the selection of
551 GAS-neutrophil association. (D) Rate of ROS production by neutrophils between 30-60 min (n=6
552 donors). (E) GAS killing by human neutrophils is inhibited at 30 min following pre-incubation
553 with actin polymerising molecule cytochalasin D (n=4 donors, Sidak's multiple comparison).
554 Results are the pooled means±SD (of triplicate measurements for panels D and E). **p<0.01,
555 ***p<0.001.

556

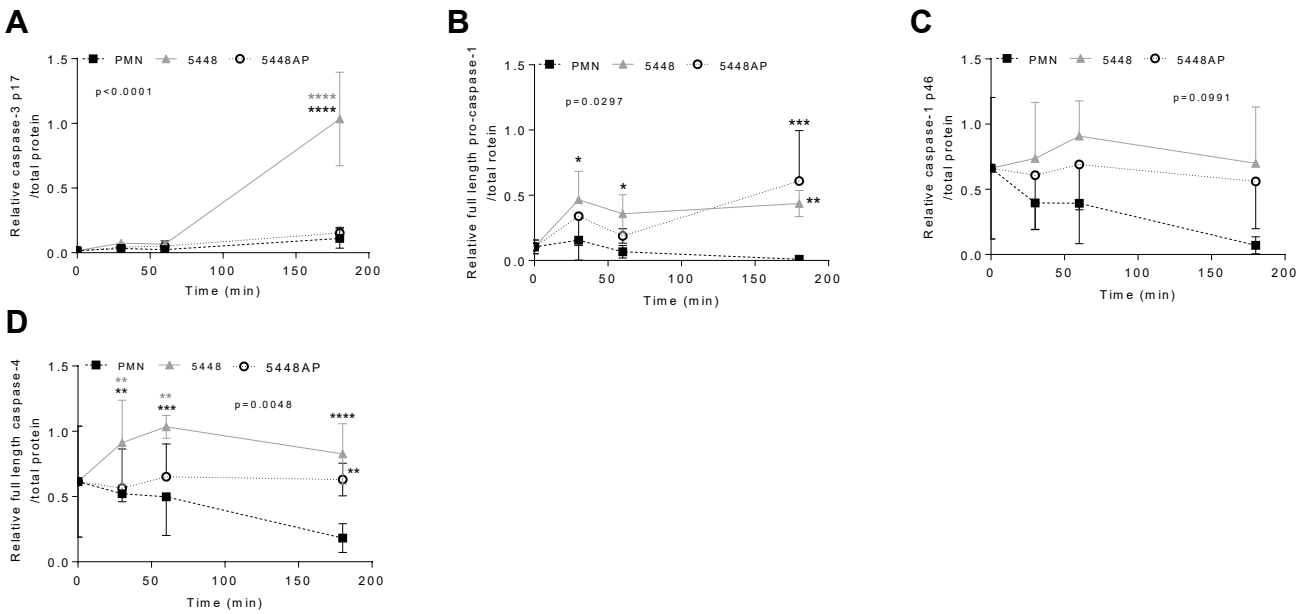

Supplementary figure 2. Quantification of protein bands in human neutrophil lysates identified through immunoblotting. (A) Caspase-3 p17, (B) caspase-1 full-length, (D) caspase-1 p46 and (D) caspase-4 immunoblots were imaged then analysed using ImageJ where area under the curve was normalised over total protein. Results are the means±SD where 3 donors were used. *p<0.05, **p<0.01, ***p<0.001 and ****p<0.0001, with black asterisks denoting significance to control and grey asterisks between 5448 and 5448AP.

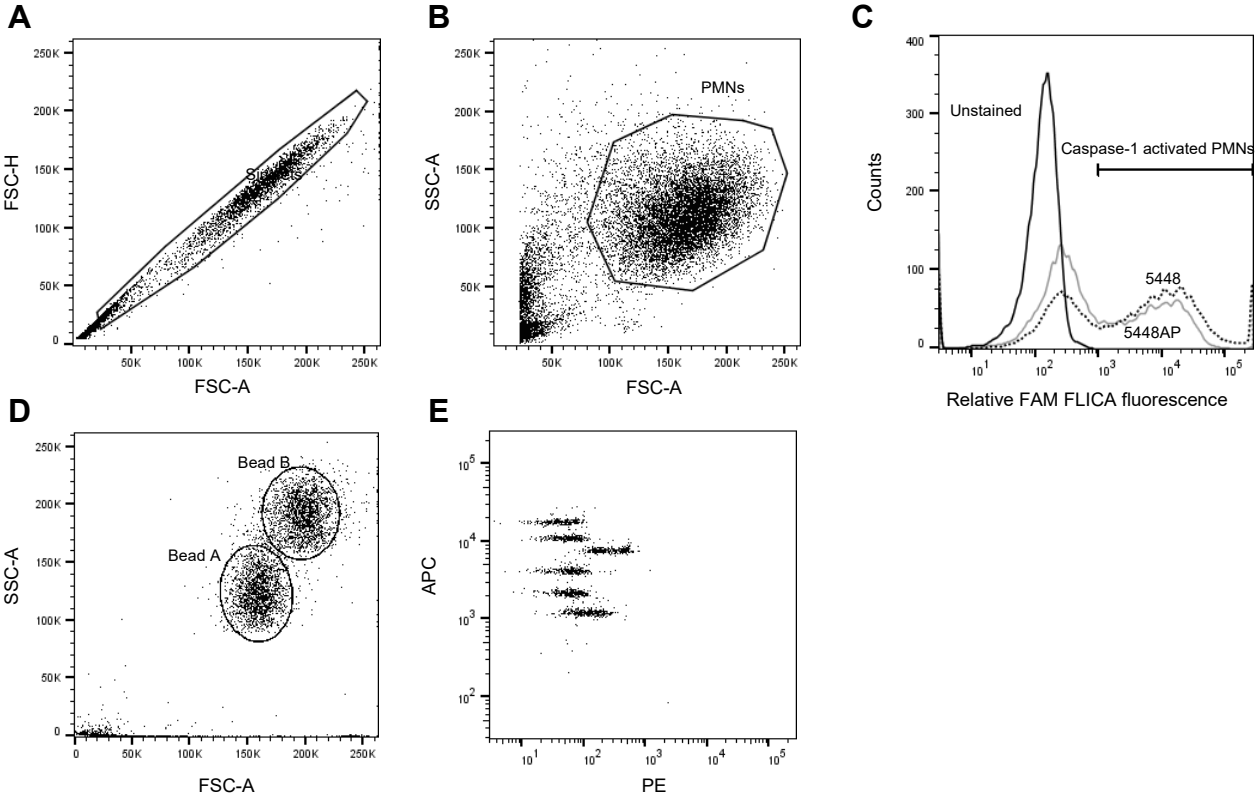

564 **Supplementary figure 3. Human neutrophils were assessed for the activation of caspase-1**
565 **and release of cytokines via and flow cytometry.** (A) Primary neutrophil (PMN) 'Singlet' cell
566 selection (FSC-A vs. FSC-H) and (B) viable 'PMNs' discrimination (FSC-A vs. SSC-A). (C)
567 Representative plot showing unstained and GAS infected neutrophils (Singlets/PMNs) with
568 FLICA (FAM-YVAD-FMK) fluorescence. Gating strategy for LEGENDplex cytometric bead assay
569 where (D) beads A and B were gated (FSC-A vs. SSC-A). Gates for beads A (shown) and B were
570 assessed for (E) PE vs. APC fluorescence where cytokines had unique APC fluorescence and
571 expression was measured via PE fluorescence when compared to a standard curve.

572

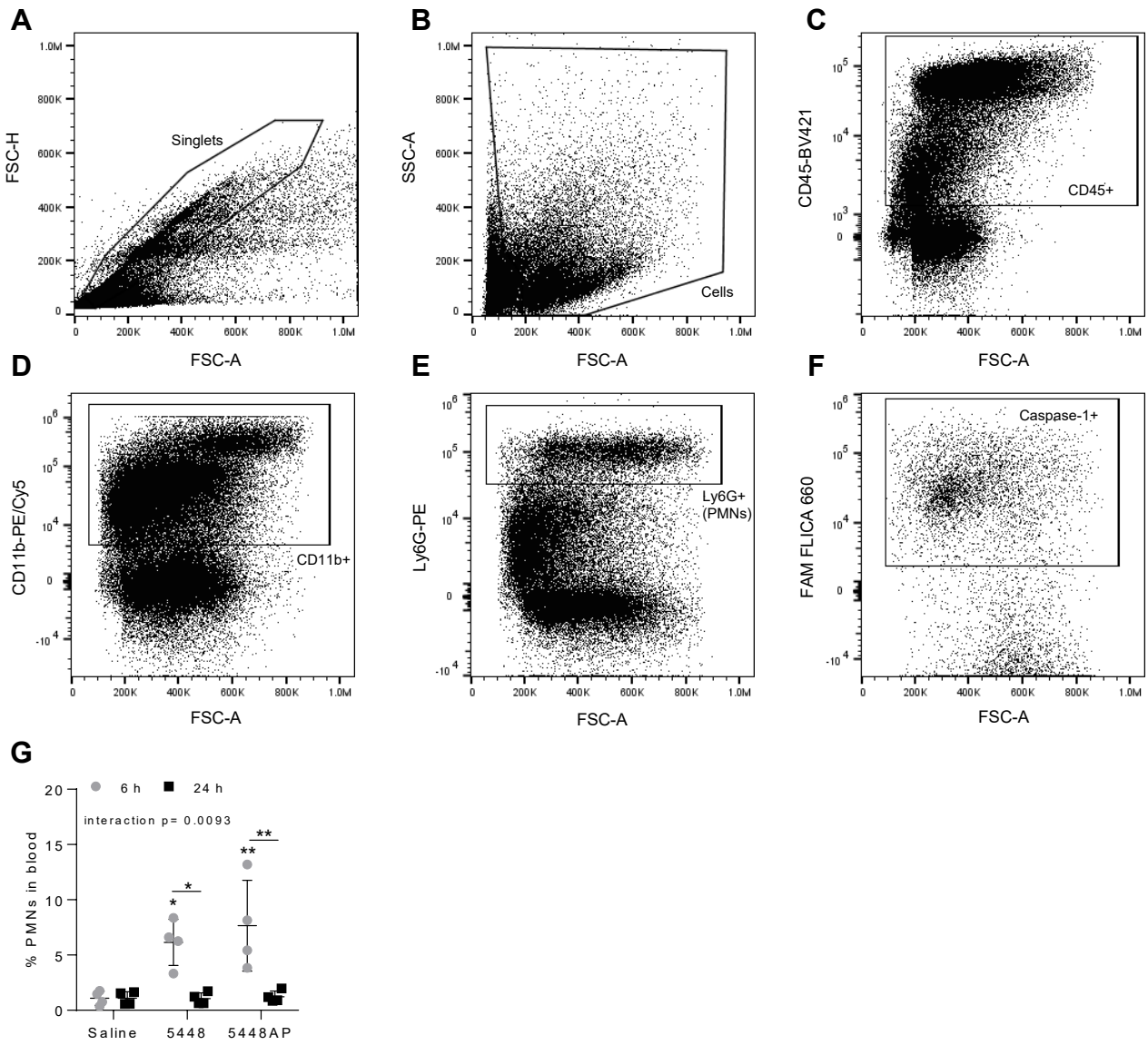

Supplementary figure 4. Flow cytometric sequential gating strategy for identification of murine neutrophils determining caspase-1 activation. (A) Primary 'Singlets' cell selection (FSC-A vs. FSC-H) and (B) 'Cells' discrimination (FSC-A vs. SSC-A) of murine blood and lavage fluid. 'Cells' were further gated upon (C) CD45-BV421 expression and (D) CD11b-PE/Cy5 expression. Neutrophils (PMNS) were defined as (E) Ly-6G-PE^{+} cells from the CD45^{+}/CD11b^{+} population. Neutrophils were assessed for (F) caspase-1 activation using FLICA 660 (660-YVAD-FMK). (G) Percentage of neutrophils (CD11b^{+}/Ly6G^{+}) of CD45^{+} leukocytes in the blood where each data point represents the result from a single mouse where n=4. Results are the means±SD. *$p<0.05$ and **$p<0.01$ where significance is depicted from control or as indicated by a line.

References

Arnaout, M. A. 1990. Structure and function of the leukocyte adhesion molecule CD11/CD18. *Blood,* 75**,** 1037-1050.

Ato, M., Ikebe, T., Kawabata, H., Takemori, T. & Watanabe, H. 2008. Incompetence of neutrophils to invasive group A streptococcus is attributed to induction of plural virulence factors by dysfunction of a regulator. *PLoS ONE,* 3.

Aziz, R. K. & Kotb, M. 2008. Rise and persistence of global M1T1 clone of Streptococcus pyogenes. *Emerging Infectious Diseases,* 14**,** 1511-1517.

Aziz, R. K., Pabst, M. J., Jeng, A., Kansal, R., Low, D. E., Nizet, V. & Kotb, M. 2004. Invasive M1T1 group A Streptococcus undergoes a phase-shift in vivo to prevent proteolytic degradation of multiple virulence factors by SpeB. *Molecular Microbiology,* 51**,** 123-134.

Boucher, D., Monteleone, M., Coll, R. C., Chen, K. W., Ross, C. M., Teo, J. L., Gomez, G. A., Holley, C. L., Bierschenk, D., Stacey, K. J., Yap, A. S., Bezbradica, J. S. & Schroder, K. 2018. Caspase-1 self-cleavage is an intrinsic mechanism to terminate inflammasome activity. *Journal of Experimental Medicine,* 215**,** 827-840.

Bratton, D. L. & Henson, P. M. 2011. Neutrophil clearance: When the party is over, clean-up begins. *Trends in Immunology,* 32**,** 350-357.

Brown, K., Brain, S., Pearson, J., Edgeworth, J., Lewis, S. & Treacher, D. 2006. Neutrophils in development of multiple organ failure in sepsis. *Lancet,* 368**,** 157-169.

Brown, S., Heinisch, I., Ross, E., Shaw, K., Buckley, C. O. & Savill, J. 2002. Apoptosis disables CD31-mediated cell detachment from phagocytes promoting binding and engulfment. *Nature,* 418**,** 200-203.

Broz, P., Von Moltke, J., Jones, J. W., Vance, R. E. & Monack, D. M. 2010. Differential requirement for caspase-1 autoproteolysis in pathogen-induced cell death and cytokine processing. *Cell Host and Microbe,* 8**,** 471-483.

Castiglia, V., Piersigilli, A., Ebner, F., Janos, M., Goldmann, O., Damböck, U., Kröger, A., Weiss, S., Knapp, S., Jamieson, A. M., Kirschning, C., Kalinke, U., Strobl, B., Müller, M., Stoiber, D., Lienenklaus, S. & Kovarik, P. 2016. Type i Interferon Signaling Prevents IL-1β-Driven Lethal Systemic Hyperinflammation during Invasive Bacterial Infection of Soft Tissue. *Cell Host and Microbe,* 19**,** 375-387.

Chatellier, S., Ihendyane, N., Kansal, R. G., Khambaty, F., Basma, H., Norrby-Teglund, A., Low, D. E., Mcgeer, A. & Kotb, M. 2000. Genetic relatedness and superantigen expression in group A streptococcus serotype M1 isolates from patients with severe and nonsevere invasive diseases. *Infection and Immunity,* 68**,** 3523-3534.

Chen, C. J., Kono, H., Golenbock, D., Reed, G., Akira, S. & Rock, K. L. 2007. Identification of a key pathway required for the sterile inflammatory response triggered by dying cells. *Nature Medicine,* 13**,** 851-856.

Cole, J. N., Barnett, T. C., Nizet, V. & Walker, M. J. 2011. Molecular insight into invasive group A streptococcal disease. *Nature Reviews Microbiology,* 9**,** 724-736.

Davies, H. D., Mcgeer, A., Schwartz, B., Green, K., Cann, D., Simor, A. E. & Low, D. E. 1996. Invasive group A streptococcal infections in Ontario, Canada. *New England Journal of Medicine,* 335**,** 547-554.

Dransfield, I., Buckle, A. M., Savill, J. S., Mcdowall, A., Haslett, C. & Hogg, N. 1994. Neutrophil apoptosis is associated with a reduction in CD16 (FcγRIII) expression. *Journal of Immunology,* 153**,** 1254-1263.

Edwards, R. J., Pyzio, M., Gierula, M., Turner, C. E., Abdul-Salam, V. B. & Sriskandan, S. 2018. Proteomic analysis at the sites of clinical infection with invasive Streptococcus pyogenes. *Scientific Reports,* 8.

Epstein, F. H. & Weiss, S. J. 1989. Tissue Destruction by Neutrophils. *New England Journal of Medicine,* 320**,** 365-376.

632 Faurschou, M. & Borregaard, N. 2003. Neutrophil granules and secretory vesicles in inflammation.
633 *Microbes and Infection,* 5**,** 1317-1327.
634 Fiebig, A., Loof, T. G., Babbar, A., Itzek, A., Koehorst, J. J., Schaap, P. J. & Nitsche-Schmitz, D. P. 2015.
635 Comparative Genomics of Streptococcus pyogenes M1 isolates differing in virulence and
636 propensity to cause systemic infection in mice. *International Journal of Medical*
637 *Microbiology,* 305**,** 532-543.
638 Fossati, G., Moots, R. J., Bucknall, R. C. & Edwards, S. W. 2002. Differential role of neutrophil Fcγ
639 receptor IIIb (CD16) in phagocytosis, bacterial killing, and responses to immune complexes.
640 *Arthritis and Rheumatism,* 46**,** 1351-1361.
641 Geering, B. & Simon, H. U. 2011. Peculiarities of cell death mechanisms in neutrophils. *Cell Death*
642 *and Differentiation,* 18**,** 1457-1469.
643 Ghimire, L., Paudel, S., Jin, L., Baral, P., Cai, S. & Jeyaseelan, S. 2018. NLRP6 negatively regulates
644 pulmonary host defense in Gram-positive bacterial infection through modulating neutrophil
645 recruitment and function. *PLoS Pathogens,* 14.
646 Greenlee-Wacker, M. C., Kremserová, S. & Nauseef, W. M. 2017. Lysis of human neutrophils by
647 community-associated methicillin-resistant Staphylococcus aureus. *Blood,* 129**,** 3237-3244.
648 Henningham, A., Döhrmann, S., Nizet, V. & Cole, J. N. 2015. Mechanisms of group A Streptococcus
649 resistance to reactive oxygen species. *FEMS Microbiology Reviews,* 39**,** 488-508.
650 Huston, J. M., Rosas-Ballina, M., Xue, X., Dowling, O., Ochani, K., Ochani, M., Yeboah, M. M.,
651 Chatterjee, P. K., Tracey, K. J. & Metz, C. N. 2009. Cholinergic neural signals to the spleen
652 down-regulate leukocyte trafficking via CD11b. *Journal of Immunology,* 183**,** 552-559.
653 Kilsgård, O., Karlsson, C., Malmström, E. & Malmström, J. 2016. Differential compartmentalization of
654 Streptococcus pyogenes virulence factors and host protein binding properties as a
655 mechanism for host adaptation. *International Journal of Medical Microbiology*.
656 Kipnis, E. 2013. Neutrophils in sepsis: Battle of the bands. *Critical Care Medicine,* 41**,** 925-926.
657 Kobayashi, S. D., Braughton, K. R., Whitney, A. R., Voyich, J. M., Schwan, T. G., Musser, J. M. & Deleo,
658 F. R. 2003. Bacterial pathogens modulate an apoptosis differentiation program in human
659 neutrophils. *Proceedings of the National Academy of Sciences of the United States of*
660 *America,* 100**,** 10948-10953.
661 Kobayashi, S. D., Malachowa, N. & Deleo, F. R. 2018. Neutrophils and Bacterial Immune Evasion.
662 *Journal of Innate Immunity,* 10**,** 432-441.
663 Kovach, M. A. & Standiford, T. J. 2012. The function of neutrophils in sepsis. *Current Opinion in*
664 *Infectious Diseases,* 25**,** 321-327.
665 Kurosaka, K., Takahashi, M., Watanabe, N. & Kobayashi, Y. 2003. Silent Cleanup of Very Early
666 Apoptotic Cells by Macrophages. *Journal of Immunology,* 171**,** 4672-4679.
667 Lamagni, T. L., Darenberg, J., Luca-Harari, B., Siljander, T., Efstratiou, A., Henriques-Normark, B.,
668 Vuopio-Varkila, J., Bouvet, A., Creti, R., Ekelund, K., Koliou, M., Reinert, R. R., Stathi, A.,
669 Strakova, L., Ungureanu, V., Schalén, C., Jasir, A., Ioannou, Y., Kriz, P., Motlova, J.,
670 Hammerum, A., Kaltoft, M. S., Iivonen, J., Loubinoux, J., Mihaila, L., Van Der Linden, M.,
671 Lütticken, R., Papaparaskevas, J., Zachariadou, L., Baldassarri, L., Orefici, G., Straut, M.,
672 Norrby-Teglund, A., Keshishian, C. & Neal, S. 2008. Epidemiology of severe Streptococcus
673 pyogenes disease in Europe. *Journal of Clinical Microbiology,* 46**,** 2359-2367.
674 Larock, C. N. & Nizet, V. 2015. Inflammasome/IL-1β responses to streptococcal pathogens. *Frontiers*
675 *in Immunology,* 6.
676 Lioy, V. S., Pratto, F., De La Hoz, A. B., Ayora, S. & Alonso, J. C. 2010. Plasmid pSM19035, a model to
677 study stable maintenance in Firmicutes. *Plasmid,* 64**,** 1-17.
678 Loh, J. M. S. & Proft, T. 2013. Toxin-antitoxin-stabilized reporter plasmids for biophotonic imaging of
679 Group A streptococcus. *Applied Microbiology and Biotechnology,* 97**,** 9737-9745.
680 Lundqvist-Gustafsson, H. & Bengtsson, T. 1999. Activation of the granule pool of the NADPH oxidase
681 accelerates apoptosis in human neutrophils. *Journal of Leukocyte Biology,* 65**,** 196-204.

682 Ly, D., Taylor, J. M., Tsatsaronis, J. A., Monteleone, M. M., Skora, A. S., Donald, C. A., Maddocks, T.,
683 Nizet, V., West, N. P., Ranson, M., Walker, M. J., Mcarthur, J. D. & Sanderson-Smith, M. L.
684 2014. Plasmin(ogen) Acquisition by Group A Streptococcus Protects against C3b-Mediated
685 Neutrophil Killing. *Journal of Innate Immunity,* 6**,** 240-250.
686 Maamary, P. G., Sanderson-Smith, M. L., Aziz, R. K., Hollands, A., Cole, J. N., Mckay, F. C., Mcarthur, J.
687 D., Kirk, J. K., Cork, A. J., Keefe, R. J., Kansal, R. G., Sun, H., Taylor, W. L., Chhatwal, G. S.,
688 Ginsburg, D., Nizet, V., Kotb, M. & Walker, M. J. 2010. Parameters governing invasive disease
689 propensity of non-M1 serotype group A Streptococci. *Journal of Innate Immunity,* 2**,** 596-
690 606.
691 Man, S. M. & Kanneganti, T. D. 2016. Converging roles of caspases in inflammasome activation, cell
692 death and innate immunity. *Nature Reviews Immunology,* 16**,** 7-21.
693 Mclaughlin, R. E. & Ferretti, J. J. 1995. Electrotransformation of Streptococci. *Methods in Molecular*
694 *Biology (Clifton, N.J.),* 47**,** 185-193.
695 Medina, E., Goldmann, O., Toppel, A. W. & Chhatwal, G. S. 2003a. Survival of Streptococcus
696 pyogenes within host phagocytic cells: A pathogenic mechanism for persistence and
697 systemic invasion. *Journal of Infectious Diseases,* 187**,** 597-603.
698 Medina, E., Rohde, M. & Chhatwal, G. S. 2003b. Intracellular survival of Streptococcus pyogenes in
699 polymorphonuclear cells results in increased bacterial virulence. *Infection and Immunity,* 71**,**
700 5376-5380.
701 Nelson, G. E., Pondo, T., Toews, K. A., Farley, M. M., Lindegren, M. L., Lynfield, R., Aragon, D., Zansky,
702 S. M., Watt, J. P., Cieslak, P. R., Angeles, K., Harrison, L. H., Petit, S., Beall, B. & Van Beneden,
703 C. A. 2016. Epidemiology of invasive group a streptococcal infections in the United States,
704 2005-2012. *Clinical Infectious Diseases,* 63**,** 478-486.
705 Nguyen, G. T., Green, E. R. & Mecsas, J. 2017. Neutrophils to the ROScue: Mechanisms of NADPH
706 oxidase activation and bacterial resistance. *Frontiers in Cellular and Infection Microbiology,*
707 7.
708 Nicholson, D. W., Ali, A., Thornberry, N. A., Vaillancourt, J. P., Ding, C. K., Gallant, M., Gareau, Y.,
709 Griffin, P. R., Labelle, M., Lazebnik, Y. A., Munday, N. A., Raju, S. M., Smulson, M. E., Yamin,
710 T. T., Yu, V. L. & Miller, D. K. 1995. Identification and inhibition of the ICE/CED-3 protease
711 necessary for mammalian apoptosis. *Nature,* 376**,** 37-43.
712 Norrby-Teglund, A., Chatellier, S., Low, D. E., Mcgeer, A., Green, K. & Kotb, M. 2000. Host variation in
713 cytokine responses to superantigens determine the severity of invasive group A
714 streptococcal infection. *European Journal of Immunology,* 30**,** 3247-3255.
715 O'grady, K. a. F., Kelpie, L., Andrews, R. M., Curtis, N., Nolan, T. M., Selvaraj, G., Passmore, J. W.,
716 Oppedisano, F., Carnie, J. A. & Carapetis, J. R. 2007. The epidemiology of invasive group A
717 streptococcal disease in Victoria, Australia. *Medical Journal of Australia,* 186**,** 565-569.
718 O'loughlin, R. E., Roberson, A., Cieslak, P. R., Lynfield, R., Gershman, K., Craig, A., Albanese, B. A.,
719 Farley, M. M., Barrett, N. L., Spina, N. L., Beall, B., Harrison, L. H., Reingold, A. & Van
720 Beneden, C. 2007. The epidemiology of invasive group A streptococcal infection and
721 potential vaccine implications: United States, 2000-2004. *Clinical Infectious Diseases,* 45**,**
722 853-862.
723 O'neill, A. M., Thurston, T. L. M. & Holden, D. W. 2016. Cytosolic replication of group a Streptococcus
724 in human macrophages. *mBio,* 7.
725 Power, C., Wang, J. H., Sookhai, S., Wu, Q. D. & Redmond, H. P. 2001. Proinflammatory effects of
726 bacterial lipoprotein on human neutrophil activation status, function and cytotoxic potential
727 in vitro. *Shock,* 15**,** 461-466.
728 Ryu, J. C., Kim, M. J., Kwon, Y., Oh, J. H., Yoon, S. S., Shin, S. J., Yoon, J. H. & Ryu, J. H. 2017.
729 Neutrophil pyroptosis mediates pathology of P. aeruginosa lung infection in the absence of
730 the NADPH oxidase NOX2. *Mucosal Immunology,* 10**,** 757-774.
731 Schneider, K. S., Groß, C. J., Dreier, R. F., Saller, B. S., Mishra, R., Gorka, O., Heilig, R., Meunier, E.,
732 Dick, M. S., Ćiković, T., Sodenkamp, J., Médard, G., Naumann, R., Ruland, J., Kuster, B., Broz,

P. & Groß, O. 2017. The Inflammasome Drives GSDMD-Independent Secondary Pyroptosis and IL-1 Release in the Absence of Caspase-1 Protease Activity. *Cell Reports,* 21**,** 3846-3859.

Skubitz, K. M., Campbell, K. D. & Skubitz, A. P. N. 1996. CD66a, CD66b, CD66c, and CD66d each independently stimulate neutrophils. *Journal of Leukocyte Biology,* 60**,** 106-117.

Sollberger, G., Strittmatter, G. E., Kistowska, M., French, L. E. & Beer, H. D. 2012. Caspase-4 is required for activation of inflammasomes. *Journal of Immunology,* 188**,** 1992-2000.

Sumby, P., Porcella, S. F., Madrigal, A. G., Barbian, K. D., Virtaneva, K., Ricklefs, S. M., Sturdevant, D. E., Graham, M. R., Vuopio-Varkila, J., Hoe, N. P. & Musser, J. M. 2005. Evolutionary origin and emergence of a highly successful clone of serotype M1 group A Streptococcus involved multiple horizontal gene transfer events. *Journal of Infectious Diseases,* 192**,** 771-782.

Sumby, P., Whitney, A. R., Graviss, E. A., Deleo, F. R. & Musser, J. M. 2006. Genome-wide analysis of group A streptococci reveals a mutation that modulates global phenotype and disease specificity. *PLoS Pathogens,* 2**,** 0041-0049.

Svensson, N., Öberg, S., Henriques, B., Holm, S., Källenius, G., Romanus, V. & Giesecke, J. 2000. Invasive group A streptococcal infections in Sweden in 1994 and 1995: Epidemiology and clinical spectrum. *Scandinavian Journal of Infectious Diseases,* 32**,** 609-614.

Tart, A. H., Walker, M. J. & Musser, J. M. 2007. New understanding of the group A Streptococcus pathogenesis cycle. *Trends in Microbiology,* 15**,** 318-325.

Tecchio, C., Micheletti, A. & Cassatella, M. A. 2014. Neutrophil-derived cytokines: Facts beyond expression. *Frontiers in Immunology,* 5.

Tran, T. a. T., Grievink, H. W., Lipinska, K., Kluft, C., Burggraaf, J., Moerland, M., Tasev, D. & Malone, K. E. 2019. Whole blood assay as a model for in vitro evaluation of inflammasome activation and subsequent caspase-mediated interleukin-1 beta release. *PLoS ONE,* 14.

Tsatsaronis, J. A., Ly, D., Pupovac, A., Goldmann, O., Rohde, M., Taylor, J. M., Walker, M. J., Medina, E. & Sanderson-Smith, M. L. 2015. Group A Streptococcus Modulates Host Inflammation by Manipulating Polymorphonuclear Leukocyte Cell Death Responses. *Journal of Innate Immunity,* 7**,** 612-622.

Tsatsaronis, J. A., Walker, M. J. & Sanderson-Smith, M. L. 2014. Host Responses to Group A Streptococcus: Cell Death and Inflammation. *PLoS Pathogens,* 10.

Valderrama, J. A., Riestra, A. M., Gao, N. J., Larock, C. N., Gupta, N., Ali, S. R., Hoffman, H. M., Ghosh, P. & Nizet, V. 2017. Group A streptococcal M protein activates the NLRP3 inflammasome. *Nature Microbiology,* 2**,** 1425-1434.

Walker, M. J., Hollands, A., Sanderson-Smith, M. L., Cole, J. N., Kirk, J. K., Henningham, A., Mcarthur, J. D., Dinkla, K., Aziz, R. K., Kansal, R. G., Simpson, A. J., Buchanan, J. T., Chhatwal, G. S., Kotb, M. & Nizet, V. 2007. DNase Sda1 provides selection pressure for a switch to invasive group A streptococcal infection. *Nature Medicine,* 13**,** 981-985.

Wang, Q., Imamura, R., Motani, K., Kushiyama, H., Nagata, S. & Suda, T. 2013. Pyroptotic cells externalize eat-me and release find-me signals and are efficiently engulfed by macrophages. *International Immunology,* 25**,** 363-372.

Wierzbicki, I. H., Campeau, A., Dehaini, D., Holay, M., Wei, X., Greene, T., Ying, M., Sands, J. S., Lamsa, A., Zuniga, E., Pogliano, K., Fang, R. H., Larock, C. N., Zhang, L. & Gonzalez, D. J. 2019. Group A Streptococcal S Protein Utilizes Red Blood Cells as Immune Camouflage and Is a Critical Determinant for Immune Evasion. *Cell Reports*.